Int. J. Heat Mass Transfer. Vol. 24, No. 12, pp. 1990–1992, 1981.
Printed in Great Britain

0017-9310/81/121990-03 $02.00/0

TOTAL TEMPERATURE–VELOCITY RELATION IN TURBULENT COMPRESSIBLE BOUNDARY LAYERS

A. J. LADERMAN*
Ford Aerospace and Communications Corp., Newport Beach, CA 92663, U.S.A.

(*Received* 6 *February* 1981 *and in revised form* 30 *April* 1981)

NOMENCLATURE

A, $= (\gamma - 1)M_\infty^2$;
h, enthalpy;
p, pressure;
Pr_m, mixed Prandtl number;
$\bar{T}$, $= (h_0 - h_w)/(h_{0_\infty} - h_w)$;
U, velocity;
x, streamwise distance;
y, distance normal to wall;
β_{k0}, $= (\delta_k/\tau_w)_0(dp/dx)$, pressure gradient parameter where subscript 0 denotes constant pressure region just upstream of adverse pressure gradient flow;
δ, boundary layer thickness;
δ_k, boundary layer velocity thickness;
ε, $= 1 - Pr_m$;
γ, specific heat ratio;
ρ, density;
τ, shear stress.

Subscripts

0, stagnation condition;
w, wall condition;
∞, free stream or edge condition;

Superscript

$\bar{}$, denotes normalization by free-value value.

THE STUDY of the total temperature–velocity profile across the compressible turbulent boundary layer has been a subject of continued technical importance for a number of years (e.g. see the work of Meier and Rotta [1], and Meier *et al.* [2]). For zero pressure gradient (ZPG) boundary layers, the classical Crocco relation $\bar{T} = \bar{U}$ is restricted to unity Prandtl number, an assumption made to eliminate the turbulent shear stress terms from the combined energy-momentum equation and permit, thereby, a simple and direct solution. Even when applied to non-unity Prandtl number flows, the linear Crocco relation offers an adequate representation for boundary layers with finite heat transfer. However, for the adiabatic case, it fails to predict the total temperature overshoot observed in numerous experiments and confirmed by the numerical analysis of Van Driest [3]. In an attempt to account for the effects of non-unity Prandtl number, Wilson [4] developed a $\bar{T} - \bar{U}$ relation based on the turbulent Reynolds analogy and an adiabatic wall temperature profile postulated earlier by Squires [5]. However, Wilson's $\bar{T} - \bar{U}$ expression does not satisfy the boundary condition $\bar{T} = 1.0$ at $\bar{U} = 1.0$. Whitfield and High [6] adopted a more rigorous approach by introducing an approximate model for the turbulent shear stress distribution into the energy-momentum equation and derived an analytical solution which provides reasonable agreement with experimental observations (e.g. see [7]). In a more recent study [8, 9] of the effects of an adverse present gradient (APG) on a supersonic turbulent boundary layer, it was found that the $\bar{T}$ vs $\bar{U}$ relation is insensitive to the pressure gradient although the shear stress distribution is apparently strongly dependent on β_{k0} (the shear stress results are described in [8], while the details of the T_0 measurements and of the $\bar{T} - \bar{U}$ relation are documented in the more comprehensive technical report [9]). It is of interest, therefore, to examine more closely the implications of the Whitfield and High solution.

The combined energy–momentum equation can be expressed as [6]:

$$\frac{d^2\bar{h}}{d\bar{U}^2} + (1 - Pr_m)\frac{1}{\tau}\frac{d\tau}{d\bar{U}}\frac{d\bar{h}}{d\bar{U}} + Pr_m(\gamma - 1)M_\infty^2 = 0 \quad (1)$$

where, using the Whitfield–High notation, the overbars represent normalization with respect to the free stream values (i.e. $\bar{h} = h/h_\infty$, $\bar{U} = U/U_\infty$). Whitfield and High assume that the Reynolds shear stress is proportional to the turbulent kinetic energy which, on the basis of an earlier study [10], leads to the following approximation for ZPG flows:

$$\frac{\tau}{\tau_w} = \frac{\rho}{\rho_w}\exp[-4(y/\delta)^{5/2}]. \quad (2)$$

With the further assumption that the velocity profile can be expressed as a power law:

$$\bar{U} = (y/\delta)^{1/m},$$

Whitfield and High show that equation (1) can be solved in terms of a power series in the form:

$$\bar{h}(\bar{U}) = \bar{h}_0(\bar{U}) + \varepsilon\bar{h}_1(\bar{U}) + \ldots \quad (3)$$

where $\varepsilon = (1 - Pr_m)$ and, with good accuracy, higher order terms in ε can be neglected.

Returning to equation (2), the density ratio (using a typical measured adiabatic wall profile for $M_\infty = 3$ and $dp/dx = 0$), the exponential term and the ratio τ/τ_w have been plotted vs y/δ in Fig. 1. It is seen that the density change across the sublayer is much larger than the change in the exponential term so that τ/τ_w reaches peak value of about 1.5 at $y/\delta \approx 0.15$. As shown in [8], the shear stress distribution in Fig. 1 is similar to that expected for $\beta_{k0} = 0.4$. In a recent study, Sanborn [11] concluded that for $dp/dx = 0$, the shear stress distribution τ/τ_w vs. y/δ is closely approximated by the exponential term in equation (2) and Fig. 1. Consequently, the Whitfield–High analysis has been repeated using the following expression for the turbulent shear stress distribution in ZPG boundary layers:

$$\frac{\tau}{\tau_w} = \exp[-4(y/\delta)^{5/2}]. \quad (4)$$

Note that at $y/\delta = 0$, equation (4) is equivalent to equation (2). Assuming again the power law velocity profile and repeating the power series solution utilized by Whitfield and

*Principal Scientist, Thermo-Fluid Dynamics Section, Aeronutronic Division.

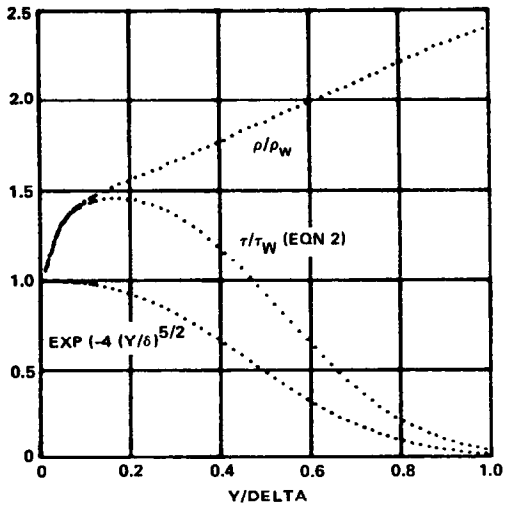

FIG. 1. Whitfield–High [6] model of turbulent shear stress distribution across the ZPG boundary layer.

High, it can be shown that to first order in ε, the solution for an adiabatic wall is:

$$\bar{T} = \bar{U}^2 \frac{\left[1 - \dfrac{8\alpha\bar{U}^2}{(\alpha+1)(\alpha+2)}\right]}{\left[\dfrac{8\alpha}{(\alpha+1)(\alpha+2)}\right]} \tag{5}$$

where $\alpha = (5/2)m$. Thus, to 1st-order, the $\bar{T} - \bar{U}$ relation is independent of both M_∞ and Pr_m although it does depend on the velocity power law exponent m. It is interesting to note that the correction introduced by expressing the turbulent shear stress distribution with equation (4) represents a departure from the Walz quadratic law [12] rather than the linear Crocco relation. To verify that the power series solution for $\bar{h}(\bar{U})$ converges rapidly, equation (1) was solved retaining terms of order ε^2. While the result for $\bar{T}$ now includes a dependence on ε, it differs from the 1st-order solution by less than 1%.

For the case of constant wall temperature (finite heat transfer), and following the same procedure used for the adiabatic case, we obtain for the $\bar{T} - \bar{U}$ relation:

$$\bar{T} = \bar{U}\left\{1 + \frac{\varepsilon}{1 + \dfrac{A}{2} - \bar{h}_w}\left[\frac{4A\alpha}{(\alpha+1)(\alpha+2)}(1 - \bar{U}^{\alpha+1}) - \frac{4}{\alpha+1}\left(1 + \frac{A}{2} - \bar{h}_w\right)(1 - \bar{U}^2) - \frac{A}{2}(1 - \bar{U})\right]\right\}. \tag{6}$$

Note that in this case, the Crocco relation $\bar{T} - \bar{U}$ is recovered when $\varepsilon = 0$. The consequences of the present solutions for $\bar{T}$ vs $\bar{U}$ will now be considered. For the adiabatic case, equation (5) is plotted in Fig. 2 for several values of m and is compared to the Whitfield–High [6] solution (for $M_\infty = 3$, $Pr_m = 0.88$, $m = 7$) and typical experimental data (for the same Mach number). It is seen that shape of the $\bar{T}$ vs $\bar{U}$ curve given by equation (5) is quite similar to the solution of Whitfield and High [6]. In addition, increasing the value of m shifts equation (5) closer to the data. A comparison of the power law velocity profile for several values of m to typical experimental ZPG adiabatic wall velocity profile data indicates that generally the power law profile does not provide a good representation of the data inasmuch as the value of m which fits the experimental profile increases with y/δ. In Fig. 2, this implies that $\bar{T} - \bar{U}$ relation shifts toward curves with increasing values of m as $\bar{U}$ increases. In view of the sensitivity of equation (5) to the exponent m it would be of interest to solve the basic equation using a more realistic velocity profile. This, however, would require a numerical solution (e.g. see [2]).

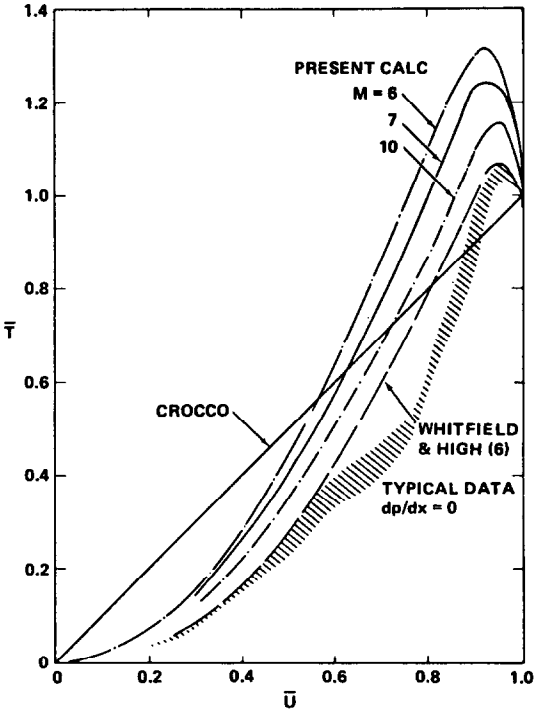

FIG. 2. Non-dimensional total temperature–velocity profiles for non-unity Prandtl number, ZPG flow adiabatic walls showing effect of exponent in velocity power law.

It should be pointed out that for the adiabatic case, the temperature difference $T_{0_\infty} - T_w$ is not large and for the present case where $M_\infty = 3$, is only about 18–20°C. The parameter $\bar{T}$ is quite sensitive to temperature and, for example, an increment of 0.1 in $\bar{T}$ represents only a 2°C change in the local total temperature. Hence, the apparently large differences in Fig. 2 correspond to only a few degrees in absolute temperature. With this in mind, it is suggested that the T_0 distribution across the boundary layer is insensitive to the model assumed for the turbulent shear stresses. This may explain why the measurements reported in [8, 9], where the

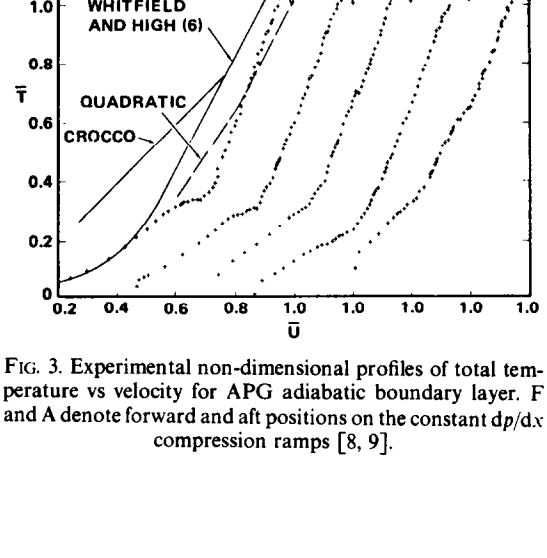

FIG. 3. Experimental non-dimensional profiles of total temperature vs velocity for APG adiabatic boundary layer. F and A denote forward and aft positions on the constant dp/dx compression ramps [8, 9].

pressure gradient is shown to produce large changes in the shear stress distribution, indicate similar results for the variation of $\bar{T}$ vs $\bar{U}$. This is illustrated in Fig. 3 where $\bar{T}$ vs $\bar{U}$ has been plotted for $dp/dx = 0$ and for forward and aft positions on the two constant dp/dx compression ramps used to generate the APG flows. The similarity in the $\bar{T}$ profiles is quite obvious and, in general, differences from the $dp/dx = 0$ case cannot be distinguished.

Before closing this discussion, it is instructive to examine the solution for the ZPG constant wall temperature case. A plot of equation (6) for $M_\infty = 3$, $Pr_m = 0.88$, $m = 7$ and several values of wall temperature is presented in Fig. 4 where it is compared to the Crocco relation, the Whitfield–High [6] solution and typical experimental data [7]. The differences between equation (6) and the solution of Whitfield and High are quite small, both are in good agreement with the data, and it is apparent that even for modest heat transfer rates (i.e. the $T_w/T_{0_\infty} = 0.71$ case) the classical Crocco relation is a good approximation to the data.

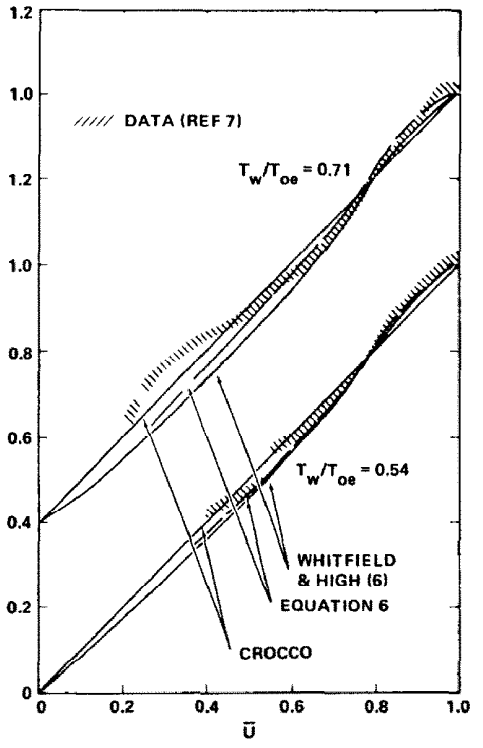

FIG. 4. Effect of heat transfer on total temperature–velocity profiles for non-unity Prandtl number, ZPG boundary layers.

Acknowledgement — This research supported by the Flight Dynamics Lab., Aeronautical Systems Division, Wright–Paterson AFB under contract F33615-77-C-3016.

REFERENCES

1. H. U. Meier and J. C. Rotta, Experimental and theoretical investigations of temperature distributions in supersonic boundary layers, AIAA Paper 70–744 (June 1970).
2. H. U. Meier, R. L. P. Voisinet and D. F. Gates, Temperature distributions using the Law of the Wall for compressible flow with variable turbulent Prandtl numbers, AIAA Paper 74–596 (June 1974).
3. E. R. Van Driest, Turbulent boundary layer in compressible fluids, *J. Aeronaut. Sci.* **18**, 145–160 (1951).
4. R. E. Wilson, Turbulent boundary layer temperature profiles and Reynolds analogy, *Int. J. Heat Mass Transfer* **21**, 1167–1170 (1978).
5. H. B. Squire, Heat transfer calculations for aerofoils, Ministry of Aircraft Production, London, R & M No. 1986 (November 1942).
6. D. L. Whitfield and M. D. High, Velocity–temperature relations for turbulent boundary layers with nonunity Prandtl numbers, *AIAA Jl* **15**, 431–434 (1977).
7. A. J. Laderman, Effect of wall temperature on a supersonic turbulent boundary layer, *AIAA Jl* **16**, 723–729 (1978).
8. A. J. Laderman, Adverse pressure gradient effects on supersonic boundary layer turbulence, *AIAA Jl* **18**, 1186–1195 (1980).
9. A. J. Laderman, Pressure gradient effects on supersonic boundary layer turbulence, Technical Report No. U-6467, Ford Aerospace and Communications Corp., Aeronutronic Division, Newport Beach, Calif. (October 1978).
10. D. L. Whitfield, Analytical, numerical, and experimental results in turbulent boundary layers, TR-76-62, Arnold Engineering and Development Center, Arnold Air Force Station, Tennessee (1976).
11. V. A. Sanborn, A review of turbulence measurements in compressible flow, NASA TMX-62337 (March 1974).
12. A. Walz, Compressible turbulent boundary layers, *Méchanique de la Turbulence*, p. 300 Centre National de la Recherche Scientifique, Paris. (1962).